

# Modeling Drone Crossing Movement with Fitts' Law

Kaito Yamada, Hiroki Usuba, and Homei Miyashita

Meiji University, Nakano, Tokyo, Japan  
kite171@me.com

**Abstract.** Drones have begun to find extensive use in commercial, scientific, recreational, agricultural, and military applications in recent times. Drone maneuvers involve several pointing and crossing operations. In this regard, previous studies have shown that drone pointing operations can be modeled by the two-part model. In this study, we conduct a crossing operation experiment to control a drone to fly through a frame with a target width. Subsequently, we verify the applicability of Fitts' law and the two-part model to drone crossing operations. Fitts' law and the two-part model are both found to be suitably valid for crossing operations ( $R^2 > 0.940$ ). Upon comparing the *AIC* values of the two models, we find that Fitts' law, which has fewer parameters, is a better model for the crossing operation. Our results indicate that the drone operation time in crossing operations can be suitably predicted. In addition, based on models, we can compare drones and evaluate interfaces in drone crossing operations.

**Keywords:** Drone, Pointing, Crossing, User performance model, Fitts' Law, Human-Drone Interaction

## 1 Introduction

Operations in graphical user interfaces (GUIs) are composed of pointing, crossing, and steering operations, and these operations have been suitably modeled. Pointing operations in GUIs involve the selection of a target (Fig. 1 left panel), whereas crossing operations involve the movement of the cursor across a boundary line (Fig. 1 right panel). The factors affecting pointing and crossing operations in GUIs are well known, and the movement time for these operations can be predicted with high accuracy by using Fitts' law. Meanwhile, steering operations in GUIs involve the movement of the cursor along a given path. Here, we note that the steering law is also derived from Fitts' law [1]. In the larger context, it has been reported that via the modeling of these operations, a general evaluation of interfaces and input devices is possible [2–5].

Against this backdrop, drone maneuvers also involve pointing and crossing operations. An example of a drone pointing operation involves directing a drone to land on a desk<sup>1</sup> (Fig. 2 left panel). Further, the use of a drone to capture a

<sup>1</sup> <https://www.tethertools.com/product/aero-launchpad/>

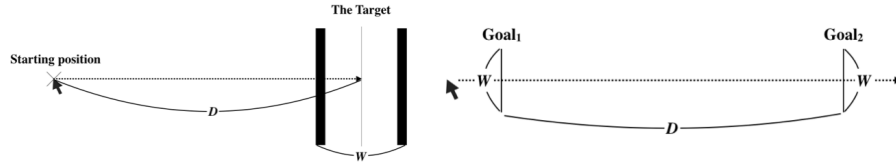


**Fig. 1.** Pointing task (left panel) and crossing task (right panel) in graphical user interfaces (GUIs)

self-portrait may also be considered as a pointing operation (Fig. 2 right panel). An example of a crossing operation is a drone race<sup>2</sup> (Fig. 3 left panel). In a drone race, the drones must pass through a frame of a certain width. As an example, the video entitled "Mirai Hikou"<sup>3</sup> shows a video shot by a drone passing through a circle formed by human arms and plastic (Fig. 3 right). Even in this scenario, the drone must pass through a frame of a certain width, i.e., this is a crossing operation. These two crossing operations can be maneuvered in the first-person view (FPV), whereas the operation of passing through a door can be executed in the third-person view (TPV). Thus, drone maneuvering involves many pointing and crossing operations. Here, we note that if these maneuvers are modeled, the operation time of the drone can be predicted. In addition, we can compare devices (such as drones and controllers) in a manner similar to GUI comparisons, and we can, for example, make a statement that "drone A can be controlled faster than drone B in this difficulty level." In addition, new drone control interfaces can be evaluated over a wide range of difficulty levels. In this regard, previous studies have already demonstrated that pointing operations can be modeled by the two-part model [6] (Fitts' law was found unsuitable). Against this backdrop, in this study, we conducted a crossing operation experiment to control a drone to fly through a frame with a target width (Fig. 4) in an attempt to model the crossing operation with both Fitts law and the two-part model.



**Fig. 2.** Examples of drone pointing operations: Landing on desk (left); Self-portrait captured by drone (right)

<sup>2</sup> <https://youtu.be/4u7C-tx2ho0>

<sup>3</sup> <https://youtu.be/2dceR6Ya79w>



**Fig. 3.** Examples of drone crossing operations: Drone race (left); Video production by drone (right)

## 2 Related Work

### 2.1 Drone maneuvering

In the FPV operation of a drone, it is difficult to accurately determine the drone height and position. In certain studies, this problem has been solved using XR [7, 8]. Further, Erat et al. proposed a TPV maneuvering system using a HoloLens to address the difficulty of maneuvering a drone from the FPV in narrow paths, as might be required in disaster scenarios [9].

Meanwhile, several other studies have explored many drone maneuvering methods and interfaces. Hall et al. investigated three maneuvering techniques and determined which among them could capture pictures in the fastest possible time (methods included maneuvering from the TPV, the FPV on a tablet, and the FPV with a headset) [10]. Further, Hansen et al. determined the optimal combination by combining eye movements and controller manipulation methods [11]. Cho et al. discussed the difficulty of users in perceiving the actual direction of a drone [12]. Kasahara et al. proposed a method to control a drone by means of a touch screen [13].

### 2.2 Modeling and Evaluating Devices

Input devices in GUIs have been evaluated in many studies; Card et al. [3] evaluated devices such as the mouse and joystick, while Ramcharitar et al. [14] have compared game controllers. Here, we again note that these devices are modeled by using Fitts' law [3, 14].

Other devices have been also modeled, such as sewing machines [15], forklifts [16], the turning of a two-handled crank [17], and driving simulators [18]. Thus, there are precedents for Fitts' law or the steering law also being suitable for operations other than those in GUIs.

### 3 Experiment

In our study, we conducted a drone crossing operation experiment to control a drone completely and fly it through a frame with a target width.

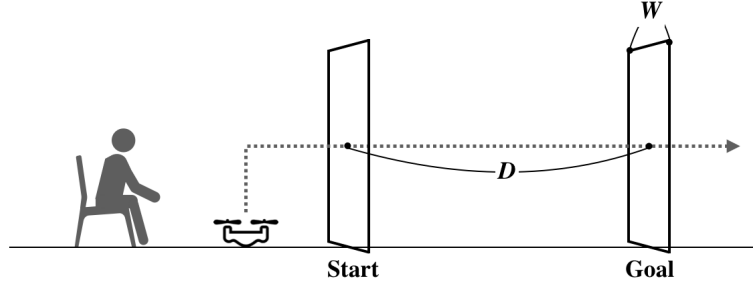


Fig. 4. Crossing experiment outline

#### 3.1 Participants

The participants of our study included 12 undergraduate and graduate students (7 male and 5 female students, average 23.2 years,  $SD = 0.80$  years). Two participants had little experience in drone control, while nine had been subjected to previous experiments conducted by us for about two hours, and one had a total of about ten hours of drone operation experience.

#### 3.2 Task

The participants were required to control a drone on a path through two frames (Fig. 4). To reduce the effect of the difference in the height of each participant, they were made to sit on a chair at a distance of 1.0 m from the starting area (Fig. 5, left panel). The participants were requested to perform the task as quickly and accurately as possible. The participants were informed that the flight position of the drone was freely adjustable until drone passage through the start frame. In this experiment, a trial was considered successful if the drone passed from the start frame to the goal frame without colliding with either frame; otherwise, it was considered to be unsuccessful. Participants were notified of their success or failure in each trial.

#### 3.3 Apparatus

The experiment was conducted in a room (6.0 m in length, 2.5 m in width, and 2.5 m in height) containing no obstacles. The air-conditioning in the room was

turned off. To prevent collision of the drone with the wall, a mat was positioned behind the goal frame (Fig. 5, left panel). A drone called "Parrot Mambo Fly (180.0 mm in length, 180.0 mm in width, 40.0 mm in height)<sup>4</sup>" was used for the experiment; this drone has a dedicated iPad application called "Free Flight Mini"<sup>5</sup> as the controller (Fig. 5 right). The speed of the drone is controlled by the inclination of the drone; the maximum inclination can be adjusted in the range of  $5^\circ$  to  $25^\circ$  in the application. We chose the default setting ( $15^\circ$ ) in the experiment.



**Fig. 5.** Crossing experiment environment: Photograph of actual experiment (left panel); Drone and controller used for experiment (right panel)

### 3.4 Design and Procedure

The target width  $W$  was 0.3, 0.4, or 0.5 m, while the target distance  $D$  was either 2.5 or 3.5 m. The frame used in the experiment was 1.8 m in height, which we believed to be sufficient for controlling and maneuvering the drone. The participants were given a time of approximately 10 min to familiarize themselves with the drone controls; we selected one condition from the six conditions ( $2D \times 3W$ ) and the participants performed the task as practice until they succeeded three times. Subsequently, they performed the task 10 times, from which experimental data was obtained. Participants repeated the above procedure six ( $2D \times 3D$ ) times. The order of selecting the conditions was counterbalanced by the Latin square. In total, 720 trials (i.e.,  $2D \times 3W \times 10$  sets  $\times$  12 participants) were conducted; the time required was approximately 40–80 min per participant.

### 3.5 Measurement

The movement time  $MT$  (the time difference between when the center of the drone passes through the start frame and when it passes through the goal frame) and error rate were recorded for each trial. Parameter  $MT$  was measured from the videos obtained during the experiments.

<sup>4</sup> <https://www.parrot.com/global/drones/parrot-mambo-fly>

<sup>5</sup> <https://www.parrot.com/global/freelflight-mini>

## 4 Results

The acquired data were analyzed by means of repeated measures ANOVA and the Bonferroni post hoc test. The data of ten trials were deleted by mistake, and hence, the data of only 710 trials were used as experimental data. The number of errors was 124 (17.4 %).

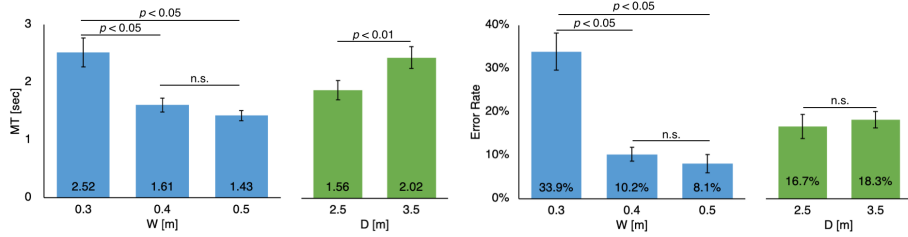


**Fig. 6.** Effects of distance  $D$  and width  $W$  on movement time  $MT$  (left panel) and error rate (right panel) in crossing experiment

### 4.1 Effects of $D$ and $W$ on $MT$

First, we examined the main effects of  $W$  ( $F_{2,22} = 25.06$ ,  $p < 0.01$ ) and  $D$  ( $F_{1,11} = 13.28$ ,  $p < 0.01$ ) on  $MT$  (Fig. 6 left panel). From multiple comparisons, it was observed that an increase in  $D$  ( $p < 0.01$ ) and/or decrease in  $W$  ( $p > 0.10$  for  $W$  values between 0.4 m and 0.5 m; otherwise,  $p < 0.05$ ) resulted in an increase in  $MT$  (Fig. 6 left). The interaction in  $D \times W$  on  $MT$  was not observed ( $F_{2,22} = 0.50$ ,  $p > 0.10$ ).

### 4.2 Effect of $D$ and $W$ on error rate

We next observed the main effects of  $W$  ( $F_{2,22} = 31.95$ ,  $p < 0.01$ ) on the error rate; however, we could not observe the main effects of  $D$  ( $F_{1,11} = 0.55$ ,  $p > 0.10$ ) on the error rate (Fig. 6, right panel). From multiple comparisons, we found that decreasing  $W$  ( $p > 0.10$  for  $W$  between 0.4 m and 0.5 m; otherwise,  $p < 0.05$ ) resulted in an increase in the error rate (Fig.6 right). The interaction in  $D \times W$  on error rate was not observed ( $F_{2,22} = 0.70$ ,  $p > 0.10$ ).

### 4.3 Model fitness

The movement time ( $MT$ ) of crossing operations in GUIs can be modeled by Fitts' law (Eq. 1); thus, Fitts' law can be considered as a candidate model. In the crossing experiment, for example, if the drone collides with the frame, the drone may crash, and therefore, it is necessary to ensure clear passage of

the drone completely within the frame. Therefore, taking into account the size of the drone ( $S = 0.18m$ ), the model in which the target width  $W$  for Fitts' law is replaced by  $W - S$  becomes a candidate model (Eq. 2, the log term of this equation is represented as  $ID_{cf}$ ). Meanwhile, a previous study [6] has demonstrated that the two-part model is also a good fit for pointing operations; thus, the two-part model also forms a candidate model (Eq. 3, the log term of this equation is represented as  $ID_{ct}$ ).

$$MT = a + b \log_2 \left( \frac{D}{W} + 1 \right) \quad (1)$$

where  $a$  and  $b$  denote the regression constants (hereafter,  $a$ ,  $b$ , and  $k$  are used as regression constants).

$$MT = a + b \log_2 \left( \frac{D}{W - S} + 1 \right) \quad (2)$$

$$MT = a + b \log_2 \left( \frac{D + (W - S)}{(W - S)^k} \right) \quad (3)$$

Next, we verified whether Fitts' law (Eq. 2) suitably fits our results. The relationship between  $MT$  and  $ID_{cf}$  is depicted in left panel of Fig. 7. We note from the figure that Fitts' law affords a good fit for the crossing operation ( $R^2 = 0.940$ ). Next, we verified whether the two-part model (Eq. 3) could suitably fit our results. The relationship between  $MT$  and  $ID_{ct}$  is shown in the right panel of Fig. 7. Again, it can be observed that the two-part model affords a good fit for the crossing operation ( $R^2 = 0.948$ ). In this regard, Shoemaker has demonstrated that when the  $MT$  curves for each  $D$  and  $W$  value do not intersect, the two-part model is more suitable than Fitts' law [19]. However, as shown in Fig. 8, the  $MT$  curves for each  $D$  and  $W$  value do overlap; thus, we can consider both Fitts' law and the two-part model to be good fits. Meanwhile, from Fig. 9, we note that the  $MT$  curves for each  $D$  and  $W$  value do not intersect in the pointing experiment.

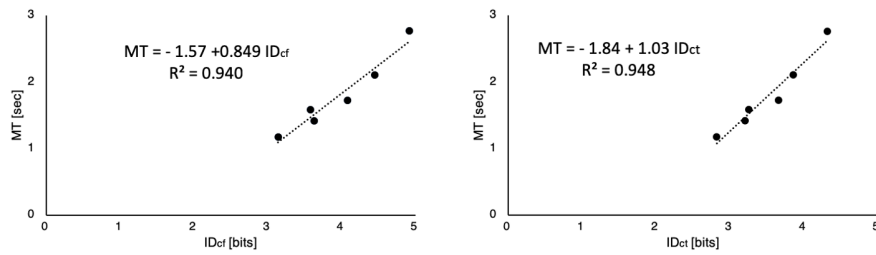


**Fig. 7.** Model suitability for Fitts' law (left panel) and two-part model (right panel) for crossing operation

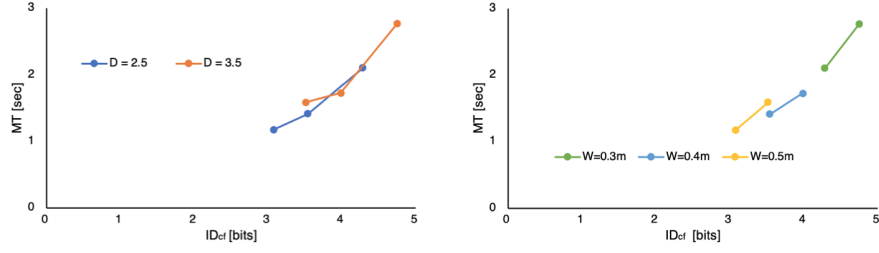


**Fig. 8.** Relationship between  $ID_{cf}$  and  $MT$  for each value of  $D$  (left panel) and  $W$  (right panel)

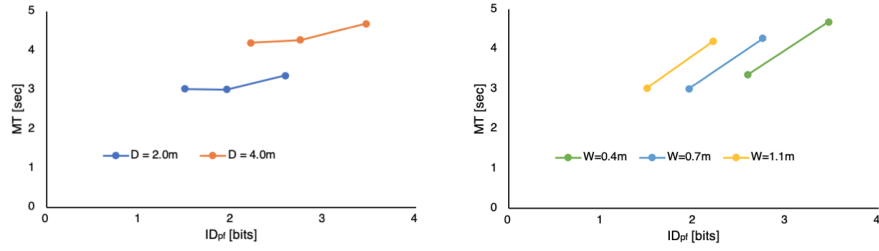


**Fig. 9.** Relationship between  $ID_{pf}$  and  $MT$  for each value of  $D$  (left panel) and  $W$  (right panel) (corresponding to Figures 11 and 12, respectively, in [6])

Tab. 1 lists the fitness of each model for the crossing operation. In general, a model with higher  $R^2$  and lower  $AIC$  is a better model. From the table, we note that  $R^2$  is slightly higher for the two-part model, whereas  $AIC$  is slightly lower for Fitts' law. Therefore, Fitts' law, which has fewer parameters, is a better model for the crossing operation.

**Table 1.** Comparison of models considered for crossing operation

|                | <i>Eq.</i>                                                 | <i>a</i> | <i>b</i> | <i>k</i> | $R^2$ | $AIC$ |
|----------------|------------------------------------------------------------|----------|----------|----------|-------|-------|
| Fitts' law     | $MT = a + b \log_2 \left( \frac{D}{W-S} + 1 \right)$       | -1.57    | 0.849    |          | 0.940 | 0.153 |
| Two-part model | $MT = a + b \log_2 \left( \frac{D+(W-S)}{(W-S)^k} \right)$ | -1.84    | 1.03     | 0.806    | 0.948 | 1.42  |

## 5 Discussions

### 5.1 Effect of target width

Participants made comments such as, “I felt that reaching the target was difficult when the width was reduced, but I did not feel it was very difficult even when the target distance was increased,” and “It was much more difficult to reach the target for narrower widths.” These comments are consistent with experimental results, wherein we observed that the error rate is affected only by the target width  $W$ . In this experiment, the target distance  $D$  was varied as 2.5 m and 3.5 m, that is, the difference was only 1.0 m; thus, it appears that more participants were affected by the width than the distance.

### 5.2 Difference in model fitness due to experimental environments

Fitts' law was found to be a good fit for the crossing operation ( $R^2 = 0.940$ ); however, it was not suitable for the pointing operation ( $R^2 = 0.672$ ) [6]. The drone used in the pointing experiment was slower than the drone used in the crossing experiment. The slower is the drone speed, the more pronounced is the effect of target distance  $D$ . The change in the  $D$  value in the crossing experiment was 1.0 m; however, the change in the  $D$  value in the pointing experiment was 2.0 m. The larger is the difference between the  $D$  values, the more will each  $D$  curve in the graph show a separation, as in the results of the pointing experiment (Fig. 9). For these reasons, for the pointing experiment, only the two-part model afforded a good fit. Therefore, even in the crossing experiments, we speculate that the two-part model will be a better fit over Fitts' law when a slower drone is used or when the gap between the  $D$  values is increased.

### 5.3 Causes of high error rates

The error rate of the crossing task was 17.4%. In this regard, participants made comments such as, “I thought that the drone had passed the frame (however, the drone had actually not reached the frame)” and “I would like to maneuver the drone from the side of the frame.” Based on these comments, we assumed that participants struggled to perceive the distance between the drone and the frame. Therefore, we considered that the error rate of this experiment is higher than the error rate of crossing on the GUI, which does not require depth perception (7.4 %) [1].

## 6 Limitation and Future work

The drone used for the experiment was prepared by experimenters, not participants. In the experiments, the drone was unlikely to break down. Further, the frame was composed of a soft material, and thus, the drone did not break down even when it collided with the frame. Moreover, we note that although we asked the participants to maneuver the drones “quickly and accurately,” when maneuvering under the risk of break down and when using their own drone, users will generally focus more on not making mistakes than reducing the movement time. That is, users will want to maneuver the drones more “accurately” than “quickly.” We considered that if the emphasizes would have been on “accuracy”, the experiment would have been closer to the actual drone operations.

Further, the user standing position and viewpoint are of importance. In this experiment, the participants stood on the takeoff side of the drone. Although there are many such situations, there are also cases in which the drone is maneuvered to return to the users or in the middle of the takeoff and the target. In the experiment, the participants maneuvered the drone while watching the target and the drone at the same time (i.e., TPV). However, as in the case of drone races, there are situations in which users need to maneuver drones from the FPV; thus, we should also verify how the FPV affects drone maneuvering. Via examining the results for various standing positions and viewpoints, we can demonstrate the effects of the standing position and viewpoints on the movement time; this will form the topic of future studies.

The steering (e.g., flying a drone through a corridor<sup>6</sup>, Fig. 10) operation forms a major component of drone operation. In GUIs, the steering law is derived from the crossing law [1]. Thus, even for drones, because crossing operations can be modeled, we hypothesize that even steering operations can be modeled.

## 7 Conclusion

In this study, we performed crossing experiments with a drone, and we studied the effects of the target distance and target width on the drone movement time

<sup>6</sup> <https://youtu.be/MI2tgUkk3Ds>



**Fig. 10.** Example of drone pointing operation: flying drone through corridor

and the error rate. Our results demonstrated that the movement time was affected by the target distance and target width, whereas the error rate was only affected by the target width. Further, an analysis of our results indicated that Fitts' law could be applied to the crossing operation. This indicates that with the use of suitable models, we can predict the drone operation time in crossing operations. In addition, we can compare various drones and controllers and evaluate the drone control interfaces in crossing operations. We believe that our findings will further contribute to advancements in drone operations across a wide range of applications.

## References

1. Johnny Accot and Shumin Zhai. Beyond fitts' law: models for trajectory-based hci tasks. In *Proceedings of the ACM SIGCHI Conference on Human factors in computing systems*, pages 295–302, 1997.
2. I Scott MacKenzie, Abigail Sellen, and William AS Buxton. A comparison of input devices in element pointing and dragging tasks. In *Proceedings of the SIGCHI conference on Human factors in computing systems*, pages 161–166. ACM, 1991.
3. Stuart K Card, William K English, and Betty J Burr. Evaluation of mouse, rate-controlled isometric joystick, step keys, and text keys for text selection on a crt. *Ergonomics*, 21(8):601–613, 1978.
4. Johnny Accot and Shumin Zhai. Performance evaluation of input devices in trajectory-based tasks: an application of the steering law. In *Proceedings of the SIGCHI conference on Human Factors in Computing Systems*, pages 466–472, 1999.
5. Masatomo Kobayashi and Takeo Igarashi. Ninja cursors: using multiple cursors to assist target acquisition on large screens. In *Proceedings of the SIGCHI Conference on Human Factors in Computing Systems*, pages 949–958. ACM, 2008.
6. Kaito Yamada, Hiroki Usuba, and Homei Miyashita. Modeling drone pointing movement with fitts' law. In *Extended Abstracts of the 2019 CHI Conference on Human Factors in Computing Systems*, CHI EA '19, pages LBW2519:1–LBW2519:6, 2019.
7. Stefanie Zollmann, Christof Hoppe, Tobias Langlotz, and Gerhard Reitmayr. Flyar: augmented reality supported micro aerial vehicle navigation. *IEEE transactions on visualization and computer graphics*, 20(4):560–568, 2014.

8. Hooman Hedayati, Michael Walker, and Daniel Szafrir. Improving collocated robot teleoperation with augmented reality. In *Proceedings of the 2018 ACM/IEEE International Conference on Human-Robot Interaction*, pages 78–86. ACM, 2018.
9. Okan Erat, Werner Alexander Isop, Denis Kalkofen, and Dieter Schmalstieg. Drone-augmented human vision: Exocentric control for drones exploring hidden areas. *IEEE transactions on visualization and computer graphics*, 24(4):1437–1446, 2018.
10. Brian D Hall, Nicolaus Anderson, and Kierstan Leaf. Improving human interfaces for commercial camera drone systems. In *Proceedings of the 2017 CHI Conference Extended Abstracts on Human Factors in Computing Systems*, pages 112–117. ACM, 2017.
11. John Paulin Hansen, Alexandre Alapetite, I Scott MacKenzie, and Emilie Møllenbach. The use of gaze to control drones. In *Proceedings of the Symposium on Eye Tracking Research and Applications*, pages 27–34. ACM, 2014.
12. Kwangsu Cho, Minhee Cho, and Jongwoo Jeon. Fly a drone safely: Evaluation of an embodied egocentric drone controller interface. *Interacting with Computers*, 29(3):345–354, 2017.
13. Shunichi Kasahara, Ryuma Niiyama, Valentin Heun, and Hiroshi Ishii. extouch: spatially-aware embodied manipulation of actuated objects mediated by augmented reality. In *Proceedings of the 7th International Conference on Tangible, Embedded and Embodied Interaction*, pages 223–228. ACM, 2013.
14. Adrian Ramcharitar and Robert J Teather. A fitts’ law evaluation of video game controllers: Thumbstick, touchpad and gyrosensor. In *Proceedings of the 2017 CHI Conference Extended Abstracts on Human Factors in Computing Systems*, pages 2860–2866. ACM, 2017.
15. M Ali Montazer, Suresh K Vyas, and Ronald N Wentworth. A study of human performance in a sewing task. In *Proceedings of the Human Factors Society Annual Meeting*, volume 31, pages 590–594. SAGE Publications Sage CA: Los Angeles, CA, 1987.
16. Colin G Drury and P Dawson. Human factors limitations in fork-lift truck performance. *Ergonomics*, 17(4):447–456, 1974.
17. Kyle Reed, Michael Peshkin, J Edward Colgate, and James Patton. Initial studies in human-robot-human interaction: Fitts’ law for two people. In *Robotics and Automation, 2004. Proceedings. ICRA’04. 2004 IEEE International Conference on*, volume 3, pages 2333–2338. IEEE, 2004.
18. Shumin Zhai and Rogier Woltjer. Human movement performance in relation to path constraint—the law of steering in locomotion. In *Virtual Reality, 2003. Proceedings. IEEE*, pages 149–156. IEEE, 2003.
19. Garth Shoemaker, Takayuki Tsukitani, Yoshifumi Kitamura, and Kellogg S Booth. Two-part models capture the impact of gain on pointing performance. *ACM Transactions on Computer-Human Interaction (TOCHI)*, 19(4):28, 2012.